J. Zool., Lond. (1993) **231,** 311–338

Intramuscular crossed connective tissue fibres: skeletal support in the lateral fins of squid and cuttlefish (Mollusca: Cephalopoda)

S. JOHNSEN AND W. M. KIER

Department of Biology, CB# 3280 Coker Hall, University of North Carolina, Chapel Hill, NC 27599-3280, USA

(*Accepted 12 December 1992*)

(With 1 plate and 10 figures in the text)

The lateral fins of cuttlefish and squid were modelled to test the hypothesis that an array of crossed connective tissue fibres embedded within the musculature of the fins provides the support required for bending and to evaluate the role of the connective tissue in elastic energy storage. Previous morphological studies showed that the fins consist of a tightly packed array of musculature similar to that found in other muscular hydrostats. However, an electromyographical study of low amplitude, low frequency fin beating found that, unlike other muscular hydrostats, synergistic muscle contractions do not provide the support required for fin bending. Three computer simulations were performed. The first, a force analysis, considered the resistance to lateral compression provided by the crossed connective tissue fibres of an unbent fin. The second, an energy minimization analysis, considered the shape and deformation of the fin when subjected to lateral compressive forces confined to either the dorsal or ventral surface of the fin. The results from these first two simulations were combined in a third simulation that calculated the upper limit for connective tissue strain as a function of the angle subtended by the arc of the fin. This last simulation suggests that the connective tissue array provides the support required. It also predicts that the connective tissue strain is slightly non-linear as a function of fin angle and that the connective tissue fibres on the concave side are considerably more strained than those on the convex side of a bent fin. Further, the original fibre angle of the connective tissue is such that the total amount of elastic energy stored in the array is parabolic as a function of fin angle, suggesting that the array may allow the fin to function as a harmonic oscillator. The 'spring stiffness' predicted by the model approximates the optimal value calculated for a harmonically oscillating fin at the frequency and wavelength observed. This suggests that elastic energy storage in the connective tissue fibre array may increase the efficiency of the fins during locomotion.

Contents

Introduction

General

Muscular hydrostats are tightly packed, three-dimensional arrays of muscle in which the muscles themselves provide the structural support required for movement. Many mammalian and lizard tongues, elephant trunks, and cephalopod appendages rely on such a system of skeletal support (Kier & Smith, 1985; Smith & Kier, 1989). The use of muscle as a support structure allows for great complexity and diversity of movement, but requires expenditure of energy not only by the musculature that is effecting movement, but also by the musculature that provides structural support.

The lateral fins of squid and cuttlefish have been shown to be muscular hydrostats (Kier, 1989), but in addition to the array of musculature there is also an intramuscular network of crossed connective tissue fibres. This paper examines the function of this network in providing support for fin movements.

Fin structure

The following description is summarized from a study of cuttlefish (*Sepia officinalis*) and squid (*Loligo forbesi*, *Sepioteuthis sepioidea*) fin morphology by Kier (1989). A transverse plane is defined here as a vertical plane perpendicular to the longitudinal axis of the animal, a parasagittal plane as a vertical plane parallel to the longitudinal axis, and a frontal plane as a horizontal plane parallel to the longitudinal axis.

The fins of cuttlefish and squid consist of tightly packed bundles of muscle fibres arranged in three mutually perpendicular orientations (Fig. 1). Transverse muscle bundles extend from the fin base to the distal margin. Dorsoventral muscle bundles extend from the dorsal and ventral connective tissue fasciae to the median fascia of the fin. Bundles of longitudinal muscle are oriented parallel to the long axis of the animal and are located directly above and below the median fascia. In the transverse muscle bundles, adjacent to the dorsal and ventral fasciae, are zones of muscle fibres with large mitochondrial cores. The difference between the fibres in these zones and the rest of the muscle fibres is similar to the difference found between analogues of 'red' and 'white' muscle described in squid mantle (Bone, Pulsford & Chubb, 1981; Mommsen *et al.*, 1981; Kier, 1989). The fibres with large mitochondrial cores will be referred to as aerobic fibres, since it is thought that they are specialized for oxidative respiration.

Birefringent connective tissue fibres with staining reactions typical of collagen are found primarily in three locations in the fin. First, connective tissue fibres are found in a loose feltwork in the plane of the dorsal, ventral and median fasciae. The fibres in the dorsal and ventral fasciae have slight preferred orientations in the transverse and longitudinal directions. The fibres in the median fascia have no preferred orientation (Kier, 1989). There are also irregularly spaced, short connective tissue fibres in the transverse muscle bundles. These fibres are aligned parallel to the transverse muscle fibres and are crimped in tissue prepared for paraffin histology. Most of the remaining connective tissue is in a crossed fibre array that is present in all three sets of muscle bundles. The fibres of this array are oriented in transverse planes at 45° to the transverse and dorsoventral muscle fibres (Fig. 1).

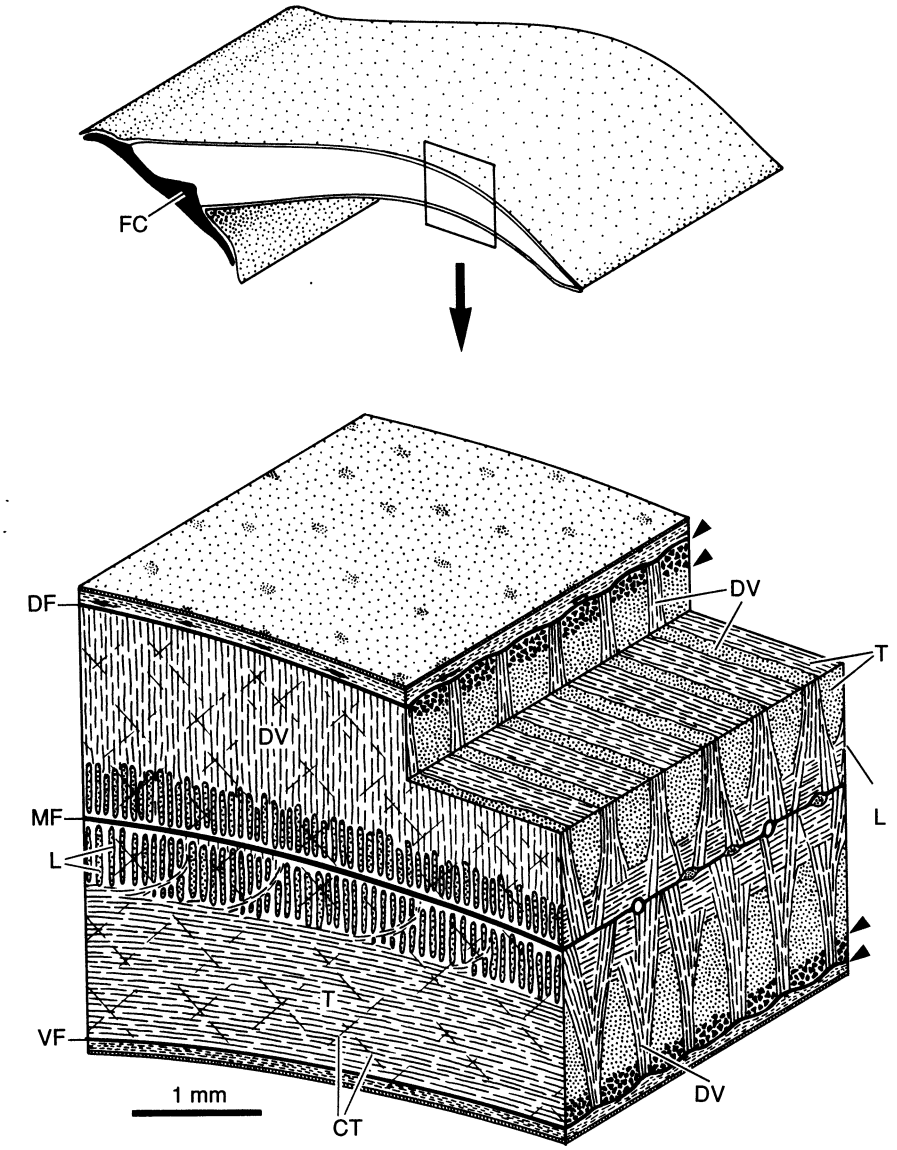

FIG. 1. Schematic diagram of the morphology of the fin of *Sepia officinalis*. DF, dorsal fascia; DV, dorsoventral muscle; FC, fin cartilage; L, longitudinal muscle; MF, median fascia; T, transverse muscle; VF, ventral fascia; CT, crossed connective tissue fibres. Arrows delimit zones of transverse muscle fibres specialized for oxidative metabolism. From Kier *et al.* (1989).

Previously proposed muscle functions

The fins operate by passing undulatory waves along their length (Plate I). In creating these waves, adjacent sections of the fin sequentially bend dorsally and ventrally. Since there are no gas-filled cavities in the fin and no displacement of fluid from the fin, the volume of the fin during

bending is constant. Therefore, a decrease in one dimension of the fin is accompanied by an increase in another. Kier (1989) proposed that bending of the fin is achieved by simultaneously contracting the transverse muscles in one half of the fin (dorsal or ventral), the dorsoventral muscles in the other half, and the longitudinal muscles in both halves. During ventral bending, the ventral transverse muscles and the dorsal dorsoventral muscles contract. The contraction of the transverse muscles laterally compresses (retracts) the ventral half of the fin. The contraction of the dorsoventral muscles reduces the thickness of the dorsal half of the fin. The longitudinal muscles prevent longitudinal extension, so the dorsal half of the fin extends laterally. The ventral lateral compression and dorsal lateral extension bends the fin ventrally. For dorsal bending, the opposite set of contractions is made.

Kier, Smith & Miyan (1989) tested these hypotheses with electromyographic recordings of the muscles of the dorsal and ventral layer and found that the situation was somewhat more complicated. *Sepia officinalis* has two distinct modes of fin activity; gentle beating and vigorous beating. Gentle beating is the usual mode and is seen in animals that are hovering or moving slowly. Vigorous beating is seen in evasive manoeuvres and prey capture and has a relatively short duration. Vigorous fin beating was found to have one and a half times the frequency and twice the amplitude of gentle fin beating (Kier *et al.*, 1989). For vigorous beating, muscle activity was observed in both the dorsal and ventral regions during both dorsal and ventral bending, supporting the proposed functions of the muscles. For gentle beating, however, muscle activity was observed only in the dorsal region during dorsal bending and only in the ventral region in ventral bending, suggesting that only the transverse muscles are active (Kier *et al.*, 1989). In addition, histological studies have shown that only the transverse muscle masses contain fibres specialized for aerobic respiration (Kier, 1989). The absence of aerobic fibres in the dorsoventral and longitudinal muscle masses suggests that these muscles do not have the aerobic capacity that is required for synergistic contraction with the aerobic transverse muscles. Thus, the dorsoventral and longitudinal muscle masses cannot provide the support required during extended gentle fin beating. Some other component of the fin must provide support. Kier (1989) proposed that the crossed fibre array of connective tissue provides this structural support. This paper tests this

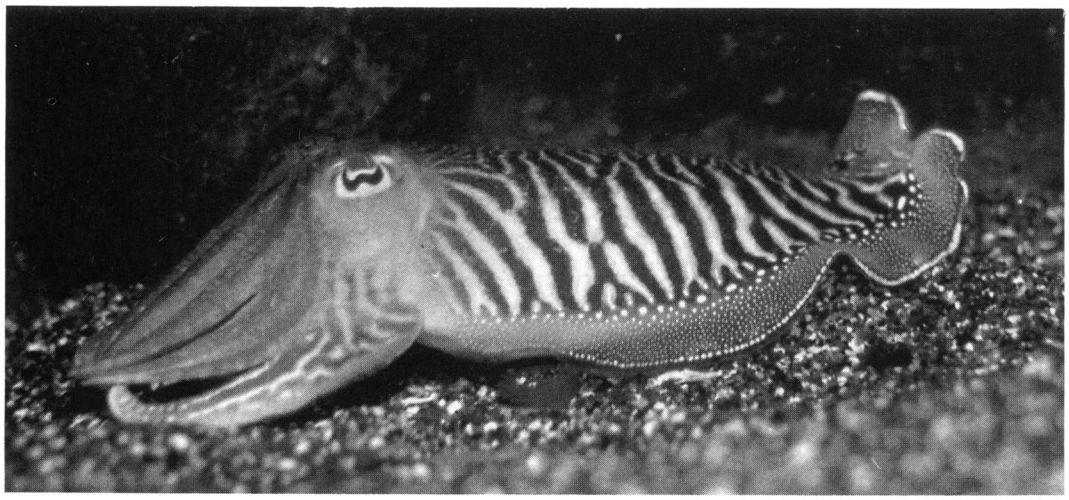

PLATE I. Photograph showing single undulatory wave on the left lateral fin of *Sepia officinalis*. From Kier (1989).

proposal using computer simulations of a geometric model, a method used in studies of reptilian tongues (Chiel *et al.*, 1992) and earthworms (Wadepuhl & Beyn, 1989).

Materials and methods

Histological techniques

Tissue samples were taken from formalin-fixed specimens of adult cuttlefish *Sepia officinalis* and adult squid *Sepioteuthis sepioidea*, embedded in either paraffin or polyester wax, cut serially in 10 μm transverse and parasagittal sections, and stained using Picro-Ponceau with Weigert Iron Haematoxylin (Humason, 1979). For details concerning anaesthesia and additional detail of histological methods, see Kier (1989). A set of serial transverse and parasagittal sections were also stained with silver for reticulum using the procedure of Naoumenko & Feigin (Humason, 1979).

Estimation of number of connective tissue fibres

The total volume of the crossed connective tissue fibres in a 10-μm section of the fin was estimated in the following way. Ten transverse sections were chosen at random from a total of 36. With the microscope slightly out of focus, an area roughly one-third of the distance from the fin base to margin was chosen. A distance of one-third was chosen because it was approximately in the centre of the region of the fin that contained the majority of the connective tissue fibres. The blurred focus, which made the fibres invisible, was used to reduce investigator bias in site choice. The focus was then sharpened and the lengths and locations of the fibres in the selected area were digitized using a camera lucida mounted on Numonics 2210 digitizing tablet. The total length, L, of the fibres and fibre fragments was measured (SigmaScan, Jandel Scientific, Corte Madera, California, USA). The total was averaged over the 10 sections chosen, and then compared to the total area, A_s, of the microscope viewing field. A transverse section of the fin was also digitized and its area, A_t, and dorsoventral length, $2t$, was calculated. The number of fibres, N_t, in one-half of the fin section is given by:

$$N_t = LA_t/(2tA_s\sqrt{2}).$$

The square root of 2 term reflects the fact that the connective tissue fibres are at a 45° angle.

Estimation of cross-sectional areas of connective tissue fibres and muscle masses

A conservative estimate of the cross-sectional area of the connective tissue was made by assuming that the fibres are cylindrical and determining their diameters from a sample of fibres viewed in a transverse section of the fin.

The relative cross-sectional areas of the different muscle masses varies with the distance from the fin base. In general, the ratio of the cross-sectional area of the longitudinal muscle mass to the cross-sectional area of the transverse and dorsoventral muscle masses increases as a function of distance from the fin base. An estimate of the cross-sectional areas of the dorsoventral, transverse and aerobic transverse muscles was made by digitizing a parasagittal fin section. The fin section chosen had approximately 20 bundles of transverse and dorsoventral muscle and was taken from approximately midway between the fin base and margin.

Estimate of active muscle tension

An estimate of peak isometric tension of cephalopod obliquely striated muscle was taken from data provided by Lowy & Millman (1962) for the funnel retractor muscle of *Sepia officinalis*.

Estimates of the various elastic moduli

A value of $5{\cdot}4 \times 10^8$ N/m^2 for the elastic modulus of cephalopod collagen was used (Gosline & Shadwick, 1983). This value is taken from the higher modulus linear portion of the stress versus strain curve. The strains experienced by the connective tissue fibres are predicted to be 1–5% (see **Results**). Although this range is within the lower modulus 'toe region' of Gosline & Shadwick's graph, the fin fibres appear straight in all sectioned material, suggesting that there is no initial pre-alignment of fibres that would give rise to a low modulus region (see Gosline & Shadwick, 1983).

An upper estimate of the elastic modulus of passive, obliquely striated cephalopod muscle was taken from a graph of stress versus strain of octopus funnel retractor muscle (Lowy & Millman, 1962). A tangent was taken at 20% strain, the highest strain recorded on the graph. Resting length was considered to be the shortest length at which a measurable tension was observed.

Computations

All calculations were done on a COMPU-ADD 286-12 microcomputer using 19 digit precision. The programming language was Microsoft C version 5·0.

The model

Construction of the model and overview of simulations

A transverse section of the fin was modelled as two vertically stacked rectangular prisms of equal size (Fig. 2a). The dimensions and number of connective tissue fibres approximate those measured in a *Sepia officinalis* fin (dorsal mantle length = 0·13 m).

The medial-lateral length of each prism is 30 times the dorsoventral length. The anterior-posterior length of each prism is many times smaller than the other two dimensions (approximately one-hundredth the dorsoventral length) and is assumed to remain constant. This assumption that the anterior-posterior length remains constant allows calculation of the upper limit of strain in the crossed connective tissue fibres (see **Discussion**). There are 120 connective tissue fibres in each prism, 60 at a 45° and 60 at a 135° angle to the bottom surface. The transverse muscles run medial to lateral. The aerobic transverse muscles comprise a fraction of the transverse muscles and are located in the bottom portion of the ventral prism and the top portion of the dorsal prism. The dorsoventral muscles run parallel to the vertical sides of each prism and are located throughout the medial-lateral length. The median fascia is the mutual boundary of the two prisms. Fin taper and the fact that the dorsal portion of the fin is slightly thicker than the ventral portion were ignored (see **Discussion**).

Note that only a thin section of the fin is modelled. As mentioned above, the fin as a whole does not bend up and down, instead, waves travel along its length. It is assumed in this paper that the entire fin can be modelled as a longitudinal array of fin sections, each section bending slightly out of phase with its neighbours.

A contraction of either the dorsal or ventral transverse muscle mass imparts both a bending and a lateral compressive force to the fin section. The kinematics resulting from the interaction of these two forces with the various tension elements in the fin is beyond the scope of this paper. The primary difficulty lies in determining the transmission of the force of the contracting muscle to the surrounding muscle tissue by shear forces. The nature and extent of this transmission has a large effect on the bending moment and the resulting kinematics of the fin section. Since it is the role of

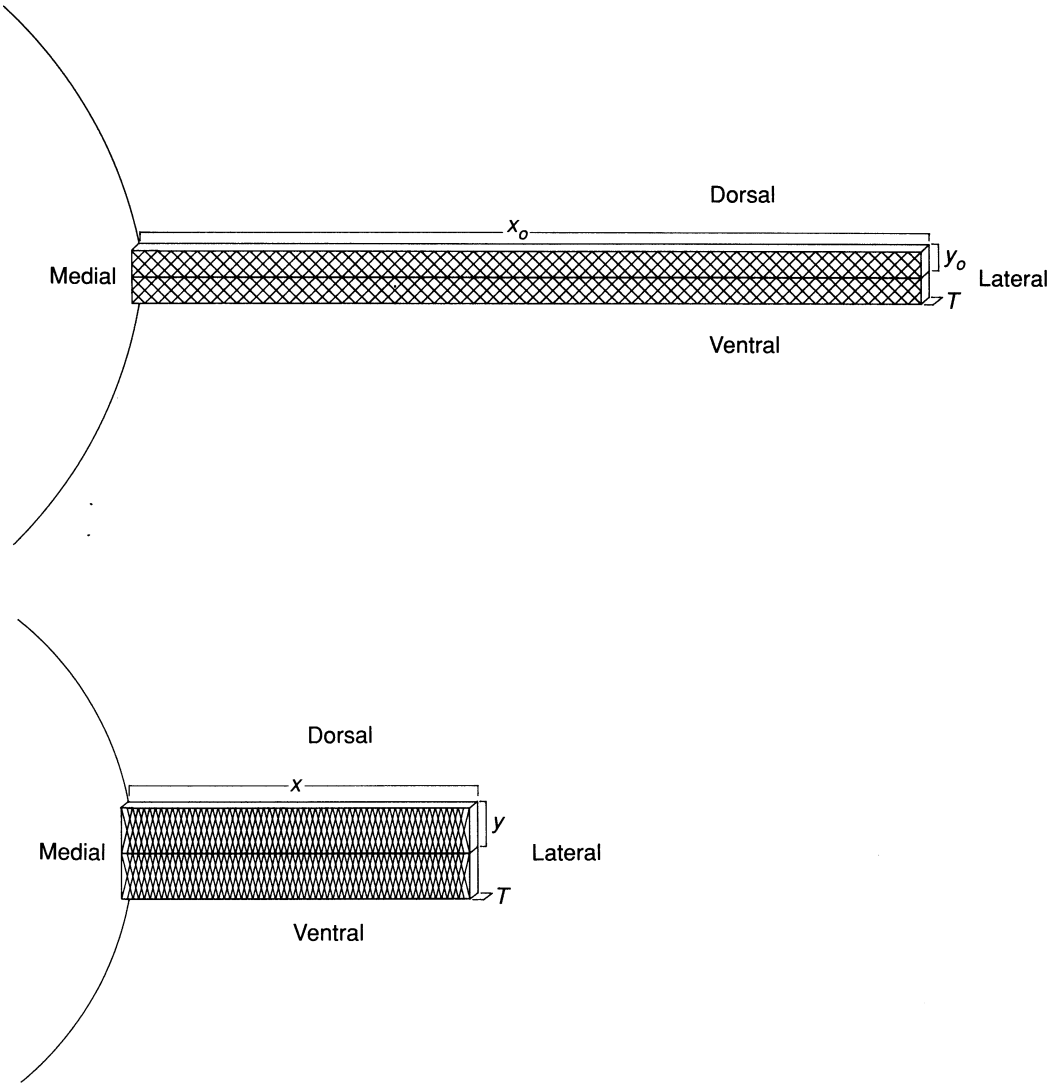

FIG. 2. (a) Schematic diagram of the model of a fin section. The curved form at the medial end of the fin represents the mantle of the animal. The various muscle masses are not shown but run as follows: transverse muscles, left–right; dorsoventral muscles, up–down; longitudinal muscles, in–out of page. x_o, y_o and T are the medial-lateral, dorsoventral, and anterior-posterior lengths of the fin section. (b) Schematic diagram of the fin model compressed to half its lateral length. The anterior-posterior length remains the same, but the dorsoventral length of the fin doubles. The lateral compression shown is exaggerated here to aid in understanding the geometry of the model. The lateral compression predicted by the model is approximately 5–10%.

the connective tissue and not the kinematics of the fin that is being examined, a simpler case was simulated. This simulation, referred to hereafter as the 'simulation of lateral compression', models the response of the fin to a lateral compressive force along the transverse axis of the fin that is evenly distributed across the fin's dorsoventral length. Compressive forces strain the fibres far

more than bending forces. Therefore, the simulation of lateral compression provides an upper estimate of the connective tissue strains and, through comparison with known maximal strains of collagen, tests the usefulness of the crossed fibre array as a skeletal support element.

Simulation of lateral compression

This simulation tests the ability of the connective tissue fibre array to resist lateral compressive forces on the fin and also determines the maximum strain in the dorsal and ventral connective tissue fibres as a function of the angle subtended by the arc of the bending fin.

The simulation involves contracting both the dorsal and ventral transverse muscle masses simultaneously, but each with only half the normal force (Fig. 2b). This results in a total muscle force equal to that produced when one of the transverse muscle masses contracts, at a given level of excitation, but without the resulting bending moment. All the muscle force is exerted in lateral compression.

There are three kinds of forces involved when the transverse muscles contract; muscular forces, pressure transduced forces, and tension in elastic elements. The compressive muscular force of the transverse muscle masses, F_h, acts in a horizontal direction and is assumed to be equally distributed over the dorsoventral length of either prism. Since the fin is a hydrostatic organ, this horizontal force creates an internal pressure, p, equal to F_h/yt, where y is the dorsoventral length of each prism and t is its thickness. Much in the way that a hydraulic brake works, this pressure transduces the horizontal force into a vertical force, F_v. $F_v=pxt$, where x is the medial-lateral length of either prism. Therefore, $F_v=F_hx/y$. Now, $xy=A_o$, where A_o is the transverse area of the uncompressed prism. So:

$$F_v=F_hx^2/A_o \tag{1}$$

The final forces considered here are tensions in the connective tissue fibres and passive dorsoventral muscle. As mentioned previously, the fibres are at a 45° angle to the dorsoventral axis. This orientation has a special property; any deformation that preserves the transverse area of the fin strains the fibres. Figure 3a shows how a simple square cross-section strains its diagonals under horizontal or vertical compression. Figures 3b and c, however, show that, for fibres other than 45°, only one of the orientations of compression strains the fibres; the other orientation places the fibres in compression. Another way of stating this is that, of all rectangular figures of a given area, the square has the shortest diagonals. It is assumed that both the connective tissue fibres and the passive muscle behave as Hookean materials; i.e. that tension $=EA\varepsilon$, where E is elastic modulus, A is cross-sectional area and ε is strain.

From Fig. 2b, it can be seen that ε_c, the strain in the crossed fibre array, and ε_{dv}, the strain in the dorsoventral muscles, can be written as:

$$\begin{aligned}\varepsilon_c &= 30\sqrt{((x/30)^2+y^2)}/(x_o\sqrt{2})-1\\ &= 30\sqrt{((x/30)^2+900A_o^2/x^2)}/(x_o\sqrt{2})-1.\\ \varepsilon_{dv} &= y/y_o-1=A_o/(xx_o)-1.\end{aligned}$$

Figure 4 shows the vertical forces acting on a small portion (1/60) of the dorsal surface of the fin. F_v is directed dorsally, and T_{dv}, the tension in the dorsoventral muscle fibres, is directed ventrally. Two connective tissue fibres, each bearing a tension, T_c, are at an angle θ to the vertical. Therefore, the total ventral force on the entire dorsal surface of the fin is:

$$120T_c\cos\theta+60T_{dv}.$$

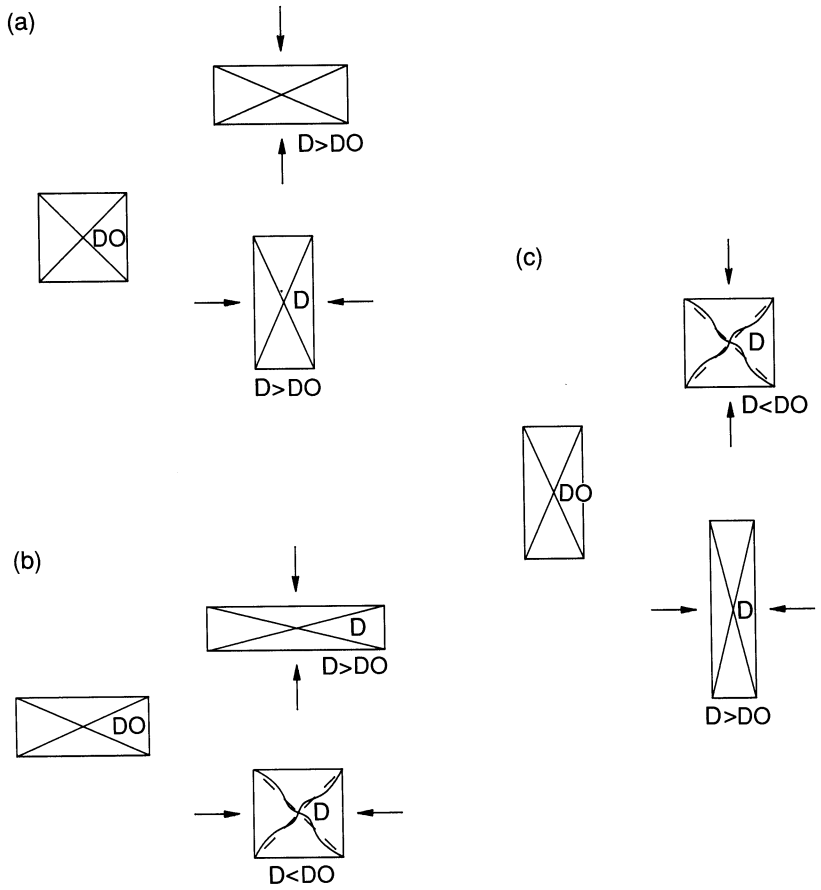

FIG. 3. Schematic diagram showing the strains of diagonal tension elements in rectangles subjected to horizontal compression or elongation. (a) Diagonals are originally oriented at 45°. Both horizontal and vertical compression strain the tension elements. (b) Diagonals are originally oriented at less than 45° to the horizontal. Horizontal compression of the rectangle results in shorter diagonals. Therefore the tension elements buckle. (c) Diagonals are originally oriented at greater than 45° to the horizontal. Vertical compression buckles the tension elements.

From Figure 2b:

$$\cos\theta = y/\sqrt{((x/30)^2+y^2)} = 30A_o/(x\sqrt{((x/30)^2+900A_o^2/x^2)}).$$

As the prisms continue to compress laterally, F_v decreases, due to its dependence on x, but the tensions in the connective tissue and dorsoventral muscle fibres increase. Also, as angle θ decreases, $\cos\theta$ increases. If, at some point, the total of the ventral forces equals the dorsal force, the fin is in equilibrium and will compress no further. The simulation searches for these equilibrium points under two different conditions: (1) the aerobic transverse muscles contract at 50% peak isometric tension; and (2) the aerobic transverse muscles contract at peak isometric tension. From (1):

$$F_v = F_h x^2/A_o.$$

$$F_h = A_{tm}s_{tm},$$

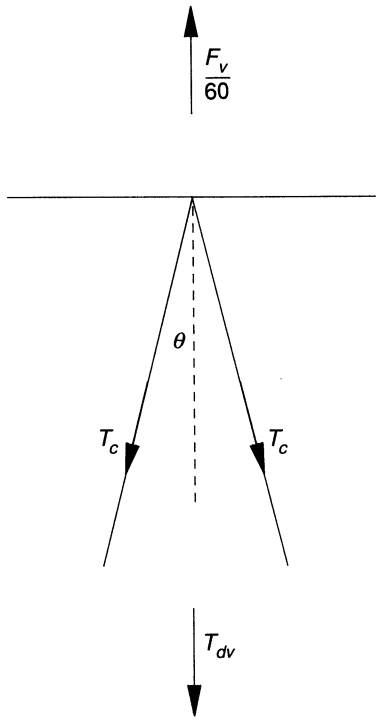

FIG. 4. Schematic diagram of the forces acting on one-sixtieth of the dorsal surface of the fin. The horizontal line is the dorsal surface. The two obliquely oriented lines are connective tissue fibres.

where A_{tm} is the cross-sectional area of the transverse muscle in one prism, and s_{tm} is half the maximum stress produced by obliquely striated muscle.

$$T_c = E_c A_c \varepsilon_c,$$

where E_c, A_c, and ε_c are the Young's modulus, cross-sectional area and strain of one connective tissue fibre.

$$T_{dv} = E_{dv} A_{dv} \varepsilon_{dv}/60,$$

where E_{dv}, A_{dv} and ε_{dv} are the Young's modulus of passive muscle and the cross-sectional area and strain of the dorsoventral muscle of either the dorsal or ventral prism.

The relevant cross-sectional areas for the transverse muscles are in the parasagittal plane (the plane perpendicular to the medial-lateral axis). In one prism, this plane has an area ty. The relevant cross-sectional area for the dorsoventral muscle is in the frontal plane (the plane perpendicular to the dorsoventral axis). It has area tx. Since the fin contains three sets of muscle bundles, the muscles of each type fill only a fraction of their cross-sectional plane. Figure 5 shows a schematic three-dimensional view of a portion of the dorsal half of the fin, showing the relevant cross-sections of the muscle masses involved. The cross-sectional area of the transverse muscle is given by:

$$A_{tm} = ty_o b_{tm},$$

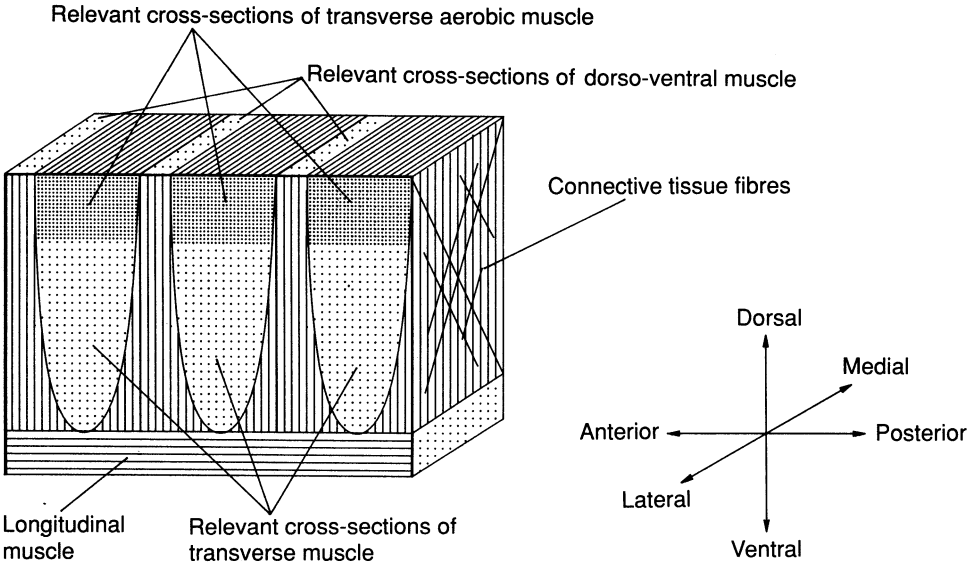

FIG. 5. Schematic diagram of a small section of the dorsal half of the fin. Note that, unlike all other figures, this diagram is oriented such that the medial-lateral axis is perpendicular to the page. The figure is a simplification of Fig. 2 and is intended only to show the relevant cross-sectional planes and areas for the strained muscle masses.

where b_{tm} is the fraction of the parasagittal plane filled by transverse muscle. The cross-sectional area of the aerobic transverse muscle is given by:

$$A_{ta} = A_{tm} b_a,$$

where A_{ta} is the cross-sectional area of the transverse aerobic muscle, and b_a is the fraction of transverse muscle that is aerobic. Therefore, the dorsal force induced when only the aerobic muscles contract is $b_a F_v$. Note that y_o rather than y is used in the estimate of the cross-sectional area. This reflects the assumption that the contractile force of a muscle bundle does not change as its cross-sectional area changes. The cross-sectional area of the dorsoventral muscle is given by:

$$A_{dv} = xtb_{dv},$$

where b_{dv} is the fraction of the frontal plane filled by the dorsoventral muscle. Since the connective tissue fibres are assumed to be cylindrical, the cross-sectional area of one fibre is given by:

$$A_c = \pi r_c^2,$$

where r_c is the radius of one fibre.

In the computer simulation, the transverse muscle contraction proceeds by increments of 0·1% of original muscle length and (if an equilibrium point has not been reached) ends when the transverse muscle is 50% of its original length.

Extension of the results from the unbent case to the bent cases

The model of a straight fin in lateral compression provides useful information on the strain

induced in the connective tissue during transverse muscle contraction, but it is also of interest to determine the strain in the connective tissue as the fin bends. Therefore, the simulation of lateral compression was extended to include an analysis of the fin as it is bent at a finite radius of curvature. The extension of the model calculates the maximum connective tissue strain for a given level of transverse muscle excitation, as a function of the angle subtended by the fin. The strains calculated represent upper limits since the extension of the model assumes that the drag of the bending fin in water is infinite.

The extension of the simulation of lateral compression is as follows. First, the fin is considered to be bent at a given radius of curvature. Then, as in the simulation of lateral compression, both the dorsal and ventral transverse muscle masses contract. The infinite drag of the fin prevents changes in the radius of curvature, so the angle subtended by the arc of the fin decreases. Again, as in the first simulation, an equilibrium will be reached between the tensions in the connective tissue and the passive dorsoventral muscle and the contractile force of the transverse muscle mass. At this equilibrium point, the strain in the connective tissue fibres and the angle subtended by the arc of the fin can be obtained. Repeating this process for radii of curvature that result in final angles ranging from zero to 90° gives the desired relation between maximal connective tissue strain and the angle subtended by the fin.

Determining the equilibrium points where the fin is bent, however, is more difficult than when the fin is straight. Various forces that cancelled in the straight case due to symmetry must now be considered. Fortunately, a simpler method than a direct force analysis exists. This method is based on the fact that a force system in equilibrium remains in equilibrium when it is mapped to another coordinate system (Kundu, 1977; Bradbury, 1984; L. E. McNeil, Dept. of Physics, University of N. Carolina, pers. comm.). Therefore, a problem that has a difficult geometry can be solved by mapping it on to a space where the geometry is simpler, solving it there, and then mapping the solution back to the original space.

An algorithm exists for finding the connective tissue and muscle fibre strains for a fin at equilibrium at a given radius of curvature. First, the fin is mapped to a space where it takes the form shown in Figure 2a. This map must be one-to-one, and must keep the transverse areas of the prisms constant. In addition, the medial-lateral length of the median fascia must also be kept constant. This final condition holds for an isotropic beam, and additional calculations provided in **Appendix I** show that it also holds for a beam containing a crossed array of fibres. After the mapping, the simulation for the unbent case is run, after which the fin appears approximately as shown in Fig. 2b. This laterally compressed fin is then mapped back to the first space using the inverse of the first map. Finally, the relevant strains are calculated.

Since the solution for the unbent case had already been computed and is always the same, the solution for any radius of curvature can be computed by using the inverse map for that radius of curvature. **Appendix II** derives this map (it is essentially the bending of a beam with a median neutral axis subject to a constant volume constraint) and calculates the strains of the connective tissue and dorsoventral muscle.

Results

Examination of fin sections gives the following geometric parameters:

$$t = 10^{-5}\ \text{m},$$
$$y_o = 8{\cdot}2 \times 10^{-4}\ \text{m},$$
$$x_o = 2{\cdot}5 \times 10^{-2}\ \text{m}.$$

Therefore, $A_o = x_o y_o = 2{\cdot}1 \times 10^{-5}$ m^2.

$$b_{tm} = 0{\cdot}50,$$
$$b_a = 0{\cdot}24,$$
$$b_{dv} = 0{\cdot}21,$$
$$r_c = 1{\cdot}3 \times 10^{-6} \text{ m}.$$

Combining these values gives:

$$A_{dv} = (2{\cdot}1 \times 10^{-6})x \text{ m}^2,$$
$$A_{tm} = 4{\cdot}1 \times 10^{-9} \text{ m}^2,$$
$$A_c = 5{\cdot}3 \times 10^{-12} \text{ m}^2,$$
$$s_{tm} = 1{\cdot}3 \times 10^5 \text{ N/m}^2,$$
$$E_{dv} = 8{\cdot}0 \times 10^4 \text{ N/m}^2,$$
$$E_c = 5{\cdot}4 \times 10^8 \text{ N/m}^2.$$

The results of the simulation of lateral compression are as follows. With the aerobic transverse muscle fibres contracting at 50% peak isometric tension, the fin laterally compresses 6·3% before equilibrium is reached. Without the connective tissue array to provide structural support, the fin would compress 22%. With the aerobic transverse muscle fibres contracting at peak isometric tension, the fin compresses 8·7% with the connective tissue and 32% without. It should be noted here that these values represent the predicted strains, assuming that the fin does not increase in anterior-posterior length. Strain in this dimension would increase the predicted compression.

The results of the extension to the bending case are summarized in the following two paragraphs. Figure 6a shows the strains in the connective tissue fibres as a function of bending in gentle fin beating when the aerobic transverse muscle fibres contract at 50% peak isometric tension. The fin goes through half a cycle, from being bent 90° dorsally to 90° ventrally. Note that the ventral fibres are strained the most in ventral bending and the dorsal fibres the most in dorsal bending. Figure 6b shows the strain energy per unit volume of the ventral connective tissue, the dorsal connective tissue, and of the two combined. Figure 7a and b show the results obtained when the aerobic transverse muscle mass contracts at peak isometric tension. These two graphs represent estimates of the upper limits of connective tissue strain and energy storage for the fin. Note that the combined strain energies in Figs 6b and 7b are parabolic with respect to fin angle.

The extension of the simulation of lateral compression to bending of the fin also provides the relation between the arc subtended by the fin and the contraction of the transverse muscle on the concave side and the strain of the transverse muscle on the convex side of the fin. When the fin subtends an arc of 90°, the transverse muscle on the concave side is contracted by 12% in gentle fin beating at 50% peak isometric tension and 15% at peak isometric tension. The transverse muscle on the convex side at this same angle is strained by 1% at 50% peak isometric tension and 3% at peak isometric tension. The strains on the convex side are smaller than the contractions on the concave side due to the initial lateral compression of the fin.

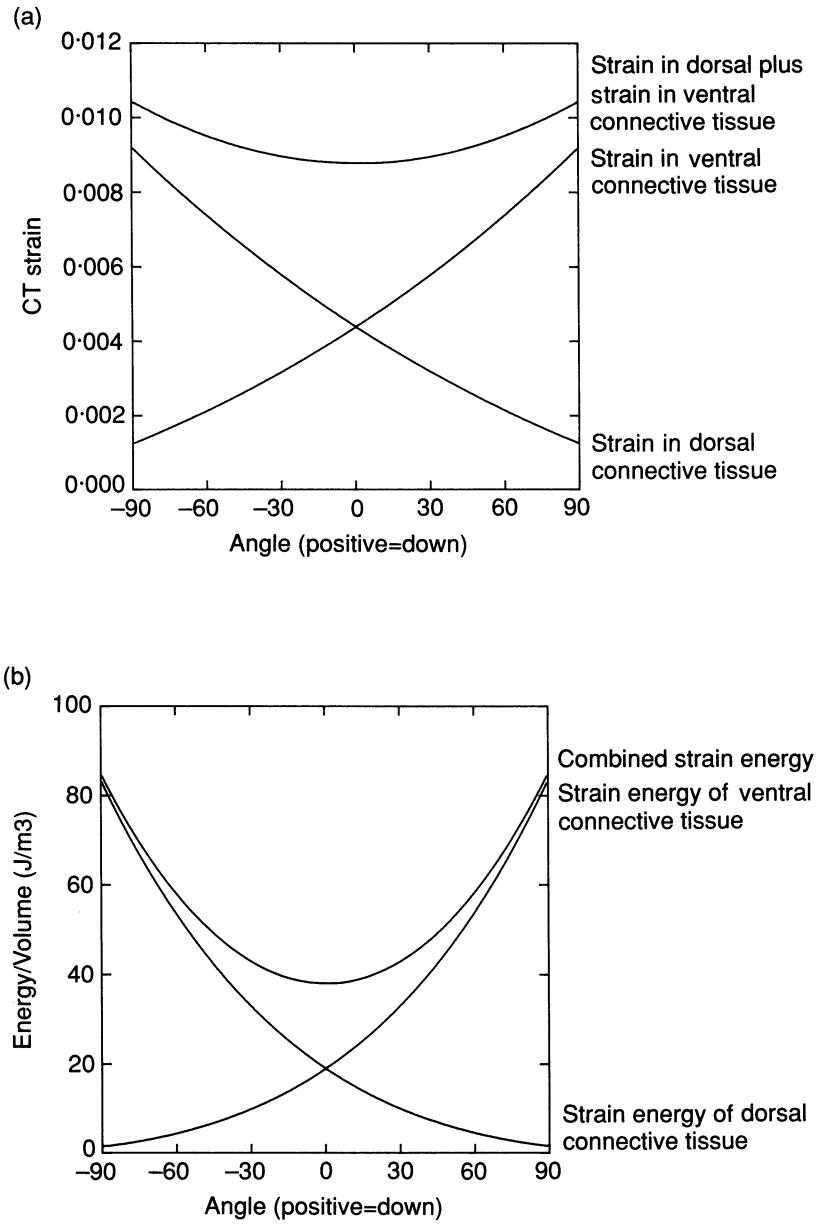

FIG. 6. (a) Graph showing connective tissue strain as a function of the angle subtended by the arc of the fin. The aerobic transverse muscle is contracting at 50% peak isometric tension. (b) Graph showing the strain energy stored per unit volume by the ventral and dorsal connective tissue array as a function of the angle subtended by the arc of the fin. The aerobic transverse muscle is contracting at 50% peak isometric tension.

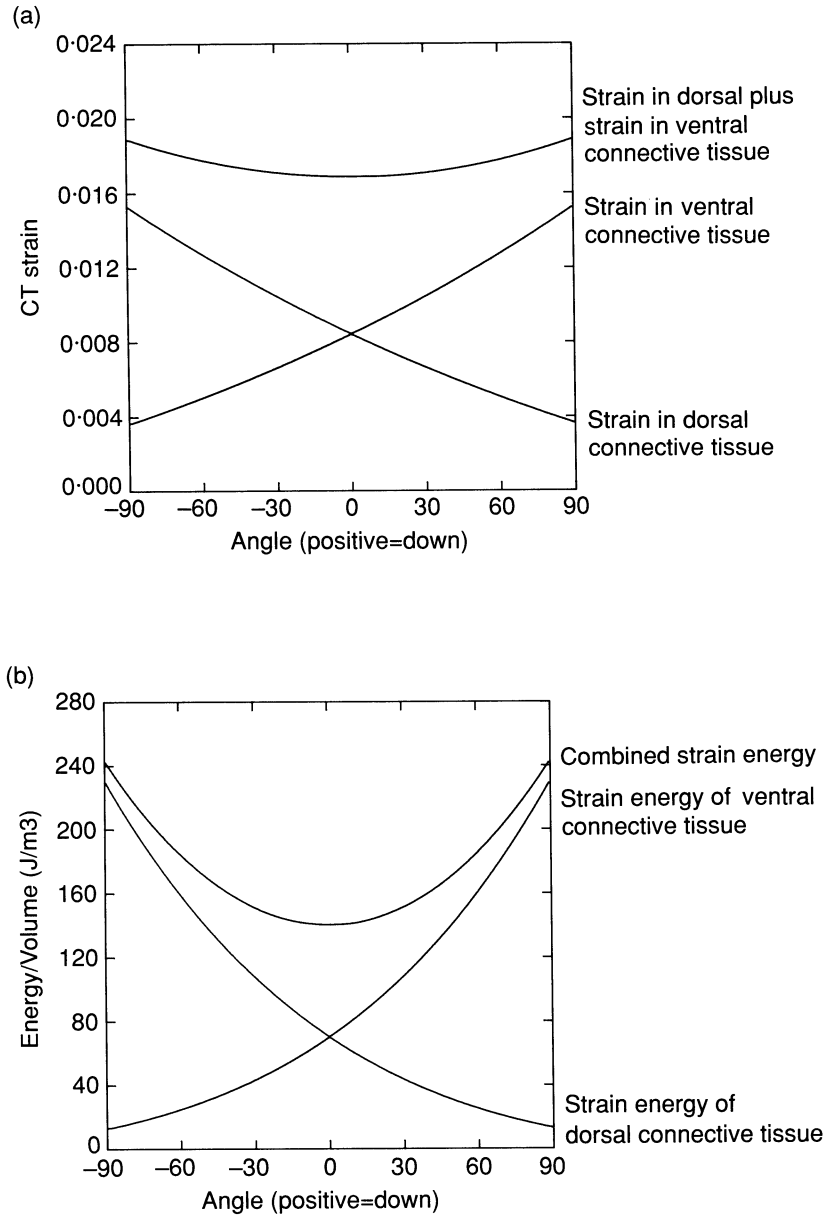

FIG. 7. (a) Graph showing connective tissue strain as a function of the angle subtended by the arc of the fin. The aerobic transverse muscle is contracting at peak isometric tension. (b) Graph showing the strain energy stored per unit volume by the ventral and dorsal connective tissue array as a function of the angle subtended by the arc of the fin. The aerobic transverse muscle is contracting at peak isometric tension.

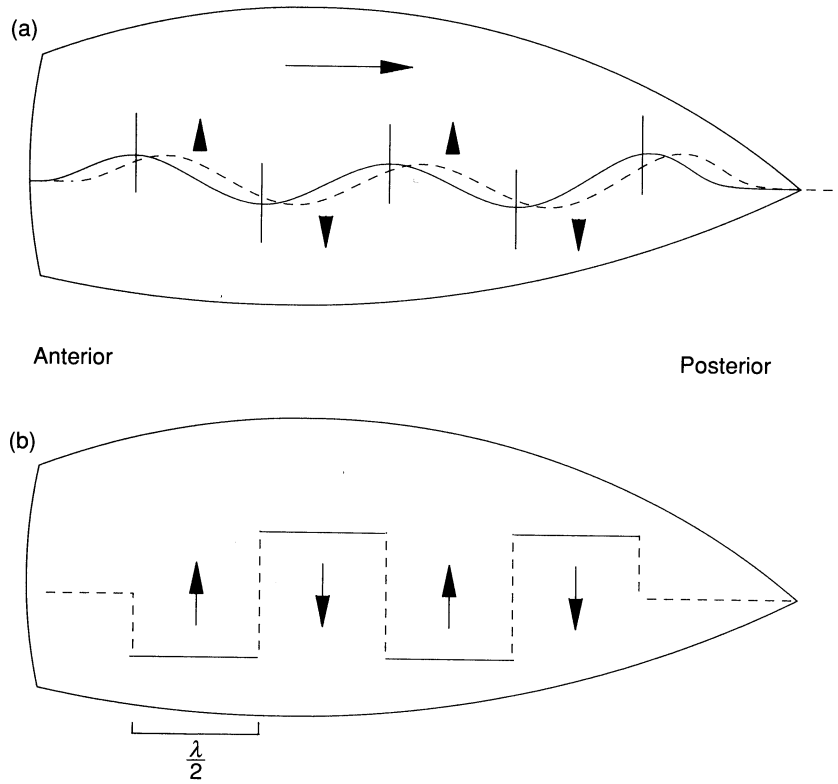

FIG. 8. (a) Schematic diagram of the mantle of a cuttlefish showing the progression of a set of undulatory waves in its lateral fin. The solid curve shows the waves at one point in time. The dotted line shows the waves a short time later. The short vertical lines divide the waves into half wavelengths from peak to trough. The vertical arrows mark the direction that the majority of the fin in a given half wavelength curves in the above-mentioned short period of time. The horizontal arrow marks the direction of the waves over time. (b) Schematic diagram depicting the approximation of the fin's motion made for the elastic energy storage calculations. For the four half wavelengths shown in (a), four fins curl up and down in isolation. Each shorter fin beats as one unit.

Discussion

Importance of support provided by connective tissue array

In this study, an upper estimate was made of the dorsoventral muscle's passive modulus and cross-sectional area, a lower estimate was made of the cross-sectional area of the connective tissue fibres, and an upper estimate was made for the forces that would be experienced during gentle fin beating. Even so, the results of the simulation of lateral compression strongly suggest that the passive muscle stresses alone cannot resist compressive force produced by the transverse muscle during bending, but that the stresses in the connective tissue array can. Therefore, the simulations predict that the connective tissue array can provide the support needed during gentle fin beating, when dorsoventral and longitudinal muscle activity is absent. During vigorous fin beating, the dorsoventral and longitudinal muscle bundles are active (see Kier *et al.*, 1989) and the support for fin bending is also provided by synergistic muscle contraction.

The extension of the simulation of lateral compression to bending of the fin predicts two other results regarding strain of connective tissue or transverse muscle. First, it predicts that connective tissue strain is slightly non-linear with respect to fin angle. Secondly, it predicts that the greatest connective tissue strain is always on the *concave* side of the fin. This is significant because previous studies of the role of connective tissue in undulatory motion have concentrated on the strains observed on the convex side of the bend (Wainwright, Vosburgh & Hebrank, 1978).

The benefits of the location of the median fascia at the neutral axis

The results of the simulation of bending (see **Appendix I**) show that the medial-lateral length of the median fascia remains essentially constant in length during muscle contraction sufficient to bend the fin 90°. All major blood vessels and nerves are found in the plane of the median fascia. These components do not tolerate large strains, so, all other things being equal, the location of the median fascia at the neutral axis of bending appears advantageous.

The advantages of an original angle of 45°

Forty-five degrees is the only angle for which the connective tissue is strained in any volume-preserving deformation. For any other original fibre angle, there exist many deformations that do not place the connective tissue in tension. The lack of strain in the fibres might at first seem advantageous in that the fin could bend without the resistance of the tensile stress of the connective tissue, but there are two important disadvantages. The first is that connective tissue oriented at other than a 45° angle cannot 'guide' the shape of the bending fin through minimization of strain energy (see **Appendix I**). If, when the transverse muscles contract, there are many deformations with zero strain energy, the resulting deformation is difficult to predict. Fin bending in this circumstance can be compared to pushing a string across a floor. A pulled string will assume a straight shape following the leading end, but a pushed string will assume any number of different shapes.

A second disadvantage of an original fibre angle other than 45° is that there is no restoring force. The role of this restoring force is discussed in the next section.

Elastic energy storage

As was seen in Figs 6b and 7b, the more the fin bends, the greater the combined strain energy of the dorsal and ventral connective tissue. Since collagen is a highly resilient material, a large percentage of the work that goes into straining the fibres can be recovered as the fin bends back towards equilibrium. This section investigates the possible use of this energy as a means of increasing the efficiency of fin beating. The chain of reasoning (excluding the Lagrangian method for determining the equations of motion) follows that described by Alexander (1988). Gentle fin beating at 50% peak isometric tension of the aerobic transverse muscles will be considered first and in greater detail; only the results are included for gentle fin beating at peak isometric tension.

Any strained solid stores energy and none does so with 100% efficiency. Therefore, stored elastic energy is ubiquitous in biology, but unless the energy can be used to increase the efficiency of the system, it will hurt rather than help the animal. One type of system that particularly benefits from stored elastic energy is a cyclical system. There are at least two ways that a cyclical system can benefit from elastic storage. In the first way, described by Wainwright *et al.* (1978), the stored

elastic energy is released at the extreme point of the cycle, when the muscles that will contract next are extended beyond their optimum length and therefore contract with less force. The transverse muscle on the convex side of the fin during beating, however, is not strained greatly (at most 3%), and it is therefore unlikely that energy savings are possible using this mechanism. A second possible productive use of stored elastic energy in cyclical systems involves natural frequencies. Elastic elements of a cyclical system oscillate with a certain natural frequency. If this frequency matches the desired frequency for the system, then large energy savings are possible. Natural frequency in harmonic oscillators is solely determined by mass and 'spring stiffness'. The spring stiffness is computed here for gentle fin beating at both 50% peak and peak isometric tension; the mass of the fin is held constant.

The remainder of this section is divided into three parts. The first describes a simple approximation for the undulating motion of the lateral fin. The second determines the equation of motion for the approximated fin and shows that it matches that of a harmonic oscillator. The final section compares the optimal 'spring stiffness' of this harmonic oscillator to that predicted by the simulation of lateral compression.

Figure 8a shows a schematic diagram of a sequence of waves passing down the length of the lateral fin of a cuttlefish. The vertical lines delimit half wavelengths. The dotted line represents the wave a short time later. Note that if the time interval is short enough, almost all of the fin in a delimited section is bending either dorsally or ventrally as a unit. To a certain extent, the water in each of these regions is isolated from the water in the other regions. The assumption for the remainder of this section is that the undulatory waves at any instant in time can be approximated as a longitudinal series of fins of length $g/2$ (where g is the wavelength of the fin beat), each short fin bending as a unit (Fig. 8b).

There is another form of Newton's laws of motion known as Lagrange's equations.

$$\mathrm{d}(\delta L/\delta \dot{q}_i)/\mathrm{d}t - \delta L/\delta q_i = 0,$$

where

$$L(q_i, \dot{q}_i) = T(\dot{q}_i) - U(q_i),$$

where $T(\dot{q}_i)$ and $U(q_i)$ are the kinetic and potential energies of the system and the q_is are the coordinates. Lagrange's equations are simply a restatement of F = ma. There are, however, two distinct advantages to their use. First, the quantities manipulated are scalars rather than vectors. Secondly, the q_is need not be rectilinear coordinates or even spatial coordinates. They can be momenta, angles, or any other quantities, as long as they are independent and fully determine the system.

Since the fin's lateral length does not change appreciably during bending (see **Appendix I**), the fin's position and shape can be entirely determined by the angle it subtends. Let this angle be ϕ. The Lagrange's equations take the form of:

$$\mathrm{d}(\delta L/\delta\, \dot{\phi})/\mathrm{d}t - \delta L/\delta\phi = 0.$$

From Appendix III,

$$T(\dot{\phi}) = ml^2\ \dot{\phi}^2/40,$$

where l is the medial-lateral length of the fin and m is the mass of both the fin and the water that moves with it. The graphs of combined strain energy in Figs 6b and 7b can be, with little error,

approximated as parabolic. Therefore, the potential energy can be represented as a function of ϕ in the following way:

$$U(\phi)=\tfrac{1}{2}\mathrm{K}\phi^2,$$

where K is a proportionality constant.
Therefore:

$$\mathrm{L}(\phi,\dot{\phi})=ml^2\ \dot{\phi}^2/40-\tfrac{1}{2}\mathrm{K}\phi^2.$$

Now,

$$\mathrm{d}(\delta L/\delta\ \dot{\phi})/\mathrm{d}t=ml^2\ \ddot{\phi}/20,$$

$$\delta L/\delta\phi=-\mathrm{K}\phi.$$

So:

$$\ddot{\phi}=-((20\mathrm{K})/(ml^2))\phi.$$

This equation has the same basic form as that of a swinging pendulum or an oscillating spring. It is the standard equation for a harmonic oscillator.

If the fin did not have to do hydrodynamic work, it would oscillate up and down with an angular velocity w given by:

$$w=\sqrt{(20\mathrm{K}/(ml^2))}. \tag{2}$$

This angular velocity, w, is known as the natural angular velocity. It is at w that all the inertial work is done by the connective tissue fibres, leaving 100% of the muscle force free to do hydrodynamic work.

Solving (2) for K gives:

$$\mathrm{K}=ml^2w^2/20.$$

As stated above, m is the mass of both the fin and the water that moves with it. Assuming that the mass of the fin is the same as that of water and that the half wavelength section of fin can be approximated as a thin plate:

$$m=((\pi/4)(g/2\mathrm{h})+1)\mathrm{pV},$$

where p is the density of water and g, h and V are the wavelength of gentle fin beating, the dorsoventral thickness of the fin, and the volume of half a wavelength of fin (see Denny (1988)).
Therefore:

$$\mathrm{K}=((\pi/4)(g/2\mathrm{h})+1)\mathrm{pV}l^2w^2/20.$$

To simplify future calculations, K/V, rather than K, will be calculated.

$$\mathrm{K/V}=((\pi/4)(g/2\mathrm{h})+1)\mathrm{p}l^2w^2/20. \tag{3}$$

The angular frequency of gentle fin beating, w, was taken from Kier *et al.* (1989). Since the specimen from which the angular frequency data were taken had a different mantle length (0·176 m) from the one that is the basis for the model in this paper (0·13 m), the dimensions of the latter specimen were linearly scaled to match that of the former. The wavelength of gentle fin beating, g, was estimated by selecting 10 random frames of a video of *Sepia officinalis*, measuring the relative lengths of one wavelength and the mantle length, taking the ratio of the two, and then linearly scaling to a specimen with a mantle length of 0·176 m.

For an animal with a mantle length of 0·176 m, w equals 6·9 radians/sec and g equals $0{\cdot}10 \pm 0{\cdot}028$ m (N = 13). Therefore:

$$K/V = 20 \times 10^3 \times (3{\cdot}3 \times 10^{-2})^2 \times (2\pi \times 1{\cdot}1)^2 \div 20$$
$$= 52.$$

This is the value predicted for K/V based on efficiency considerations. The predicted value of K/V for the fin using the simulation of 50% peak isometric tension of the aerobic transverse muscles can be obtained by assuming the combined energy curve in Fig. 6b is parabolic, locating two points on it and solving for the proportionality constant. Using zero and $\pi/4$ radians as the two points gives:

$$K/V = 38.$$

The value taken from peak isometric tension, Fig. 7b, is:

$$K/V = 78.$$

Thus, values for volume-normalized spring stiffness predicted by the simulations of lateral compression at 50% peak isometric tension and at peak isometric tension for the aerobic transverse muscle bracket the optimal value calculated from the consideration of efficiency of elastic energy storage. While this suggests that the crossed connective tissue fibre array may provide the fin with elastic properties that increase the efficiency of fin movement, further work is necessary in order to demonstrate that the assumptions of the model are valid. In particular, the assumption of constant fin length affects the values of spring stiffness calculated, since it implies that the fin is infinitely stiff in the longitudinal dimension. Although the base of the fin is attached to a stiff cartilaginous plate and the dorsal, median and ventral connective tissue fasciae resist elongation, these components obviously are not infinitely stiff. Strain in the longitudinal dimension will decrease the values of spring stiffness calculated for the fin, and thus, an accurate estimate of spring stiffness awaits future work on the mechanical properties of the fasciae and the fin as a whole. In addition, because of the inverse relationship between force and velocity of muscle contraction, the maximum force produced by the aerobic transverse muscles during fin beating will certainly be less than the upper limit set by the calculations at peak isometric tension.

The calculations described above suggest that an increase in efficiency may be possible but we cannot yet evaluate the magnitude of this potential increase in efficiency. Of critical importance is estimation of the ratio of the inertial work of the fin to the hydrodynamic work of the fin, because the larger the ratio the greater the savings (Alexander, 1988). Although the calculations described above can be used to estimate the inertial work of the fin, a more extensive analysis is required in order to calculate the hydrodynamic work of the fin.

Stereotyped motion as a condition for passive skeletal support

A feature of gentle fin beating that makes passive fibre support and elastic energy storage possible is the stereotyped nature of the motion. The fibres are positioned to support dorsal and ventral bending only. A network of this type would be of little use in appendages that undergo complex and variable movements. Crossed connective tissue fibres oriented at a specific fibre angle have not been found in the musculature of the arms and tentacles of cephalopods (Kier, 1982, 1987, 1988; Kier & Smith, 1985). Crossed fibres oriented at several different original angles have been found in squid mantle, octopus suckers, shark skin and worm cuticle, all organs or tissues

that undergo repetitive, stereotyped motions (Clarke & Cowey, 1958; Wainwright *et al.*, 1978; Kier & Smith, 1991).

Limitations of the model

Since the focus of the investigation was to determine whether the crossed fibre array could support and improve the efficiency of fin beating, modelling of certain features of the fin was not included. Fin taper was ignored. The thinner the fin is, the more it will bend for a given difference in medial-lateral length between the dorsal and ventral surfaces. Therefore, a tapered fin, given equal transverse muscle contraction along the medial-lateral length, bends not into an arc but into a logarithmic spiral. This latter shape more closely approximates what is seen in living specimens. Since the role of the connective tissue of the fin was under investigation, rather than the kinematics, the simulation was simplified by not including fin taper.

Stresses resulting from compressive muscle strains were also ignored. Little work has been done on determining the compressive modulus of resting muscle. It is doubtful, however, that inclusion of compressive stresses would significantly change the kinematics of the model. Most likely, the compressive modulus is not greater than the passive tensile modulus, and since inclusion of passive muscle tension did not greatly affect the kinematics, it is assumed that addition of compressive muscle stresses would not either.

An assumption was made that the transverse muscle masses contract equally along their lengths. This need not be the case. Histological studies (Kier, 1989) revealed that, as the fin tapers, transverse muscle fibres insert on the median fascia such that the cross-section of the transverse muscle decreases from the base to the lateral margin of the fin. Therefore, localized contraction of the transverse muscle may be possible. This could affect the shape of the fin during bending. Since the focus of the analysis was on the role of the connective tissue fibres, rather than the details of the shape of the fin in bending, the simulations assumed equal contraction along the length.

Summary

The lateral fins of cuttlefish and squid were modelled as a geometric array of tension elements. Using this model, a force analysis was done to determine the importance of an intramuscular crossed fibre array of connective tissue in resisting the lateral compression forces that are exerted during fin beating. First, the analysis considered the lateral compression of an unbent fin. Then, an energy minimization analysis was done to determine the kinematics of bending when all lateral compressive forces were confined to either the dorsal or ventral surface of the fin. The results from these first two simulations were combined to determine the maximum connective tissue strain as a function of the angle subtended by the arc of the fin. This final analysis suggests that the connective tissue array provides the support needed during gentle fin beating. Further, the results predicted that the original fibre angle of the connective tissue is such that the total amount of elastic energy stored in the array is parabolic with respect to fin angle, suggesting that the array may allow the fin to function as a harmonic oscillator. The range of 'spring stiffness' predicted by the model approximates the optimal value calculated based on the natural frequency of the fin. Thus, the connective tissue array may serve as an elastic energy storage system, increasing the efficiency of fin beating. The repetitive, stereotyped nature of fin beating is noted as a condition necessary for this form of passive support and elastic storage. Finally, the restrictions of the model are discussed.

The authors are grateful to J. M. Gosline, J. H. Hebrank, K. K. Smith and A. M. Smith for helpful comments on the manuscript and to L. E. McNeil for advice and assistance with the coordinate transforms. This research was supported by a National Science Foundation Presidential Young Investigator Award (DCB-8658069) to WMK and a National Science Foundation Predoctoral Fellowship to SJ.

REFERENCES

Alexander, R. M. (1988). *Elastic mechanisms in animal movement*. New York: Cambridge University Press.

Bone, Q., Pulsford, A. & Chubb, A. D. (1981). Squid mantle muscle. *J. mar. Biol. ass. U.K.* **61:** 327–342.

Bradbury, T. C. (1984). *Mathematical methods with applications to problems in the physical sciences*. New York: John Wiley & Sons.

Clarke, P. E. & Cowey, J. B. (1958). Factors controlling the change of shape of certain nemertean and turbellarian worms. *J. exp. Biol.* **35:** 731–748.

Chiel, H. J., Crago, P., Mansour, J. M. & Hathi, K. (1992). Biomechanics of a muscular hydrostat: a model of lapping by a reptilian tongue. *Biol. Cybern.* **67:** 403–415.

Denny, M. W. (1988). *Biology and the mechanics of the wave-swept environment*. Princeton, NJ: Princeton University Press.

Gosline, J. M. & Shadwick, R. E. (1983). The role of elastic energy storage mechanisms in swimming: an analysis of mantle elasticity in escape jetting in the squid, *Loligo opalescens*. *Can. J. Zool.* **61:** 1421–1431.

Humason, G. L. (1979). *Animal tissue techniques*. 4th edn. San Francisco: W. H. Freeman & Co.

Kier, W. M. (1982). The functional morphology of the musculature of squid (Loliginidae) arms and tentacles. *J. Morph.* **172:** 179–192.

Kier, W. M. (1987). The functional morphology of the tentacle musculature of *Nautilus pompilius*. In *Nautilus: the biology and paleobiology of a living fossil*: 257–269. Saunders, W. B. & Landman, N. H. (Eds). New York: Plenum.

Kier, W. M. (1988). The arrangement and function of molluscan muscle. In *The Mollusca, form and function* **11:** 211–252. Trueman, E. R. & Clarke, M. R. (Eds), Wilbur, K. M. (Ed.-in-Chief). New York: Academic Press.

Kier, W. M. (1989). The fin musculature of cuttlefish and squid (Mollusca, Cephalopoda): morphology and mechanics. *J. Zool., Lond.* **217:** 23–38.

Kier, W. M. & Smith, A. M. (1991). The morphology and mechanics of octopus suckers. *Biol. Bull. mar. biol. Lab. Woods Hole* **178:** 126–136.

Kier, W. M. & Smith, K. K. (1985). Tongues, tentacles and trunks: the biomechanics of movement in muscular hydrostats. *Zool. J. Linn. Soc.* **83:** 307–324.

Kier, W. M., Smith, K. K. & Miyan, J. A. (1989). Electromyography of the fin musculature of the cuttlefish *Sepia officinalis*. *J. exp. Biol.* **143:** 17–31.

Kundu, P. K. (1977). *Fluid mechanics*. New York: Academic Press.

Lowy, J. & Millman, B. M. (1962). Mechanical properties of smooth muscles of cephalopod molluscs. *J. Physiol.* **160:** 353–363.

Marion, J. B. (1970). *Classical dynamics of particles and systems*. 2nd edn. New York: Academic Press.

Mommsen, T. P., Ballantyne, J., MacDonald, D., Gosline, J. M. & Hochachka, P. W. (1981). Analogues of red and white muscle in squid mantle. *Proc. natn. Acad. Sci. U.S.A.* **78:** 3274–3278.

Smith, K. K. & Kier, W. M. (1989). Trunks, tongues and tentacles: moving with skeletons of muscle. *Am. Sci.* **77:** 28–35.

Wadepuhl, M. & Beyn, W. J. (1989). Computer simulations of the hydrostatic skeleton. The physical equivalent, mathematics and application to worm-like forms. *J. theor. Biol.* **136:** 379–402.

Wainwright, S. A., Vosburgh, F. & Hebrank, J. H. (1978). Shark skin: function in locomotion. *Science, Wash.* **202:** 747–749.

Appendix I

Energy minimization argument to show that an isotropic beam of symmetrical cross-section containing a crossed fibre array oriented at 45° bends with a median neutral axis

An isotropic beam of symmetrical cross-section bends up and down with a neutral axis that is exactly halfway between its upper and lower surfaces. The following simulation, referred to hereafter as the 'simulation of bending', tests whether the fin model also bends in this way.

In the simulation of bending, only the ventral transverse aerobic muscle mass contracts. All compressive forces are assumed to be confined to the ventral surface of the ventral prism. Due to the symmetries of the model, the fin section bends into a circular arc. For a given medial-lateral length of the aerobic transverse muscle, there exists an infinite number of arcs, each with a different medial-lateral median fascia length. The arc that would actually be observed can be predicted using Hamilton's Principle.

Hamilton's Principle

Hamilton's Principle states that any system takes the path such that the time integral of the difference between the potential and kinetic energies is minimal (Marion, 1970). If the range of kinetic energies possible is negligible in comparison to the range of potential energies possible, then the system is called quasi-static. A quasi-static system behaves such that the potential energy at any moment is minimal. A rope tied at one end to a tree and held at the other end by a person slowly walking to the tree is an example of a quasi-static system. At any moment, the rope will hang in the shape that has the least gravitational potential energy. Note that the rope takes the lowest energy state possible subject to its constraints; it cannot lie on the ground because it is being held at both ends. Hamilton's Principle allows one to determine the kinematics of a system without having to manipulate force vectors.

For the purpose here, gentle fin beating in cuttlefish is assumed to be a quasi-static system. Since the fin is essentially neutrally buoyant, the relevant potential energies are not gravitational, but stored in the strains of elastic materials. An earlier run of this simulation that included passive muscle tension was indistinguishable from a run without, so for clarity of explanation, connective tissue will be the only elastic element considered. Therefore, for any given radius of curvature, the fin is shaped such that the energy stored in the connective tissue is minimal. Assuming that the connective tissue acts as a Hookean material, the potential energy, U, is given by:

$$U = \mathrm{K}(\varepsilon_{ctv}^2 + \varepsilon_{ctd}^2),$$

where K is a proportionality constant and ε_{ctv} and ε_{ctd} are the strains of the ventral and dorsal connective tissue fibres, respectively.

With trigonometry and algebra (see **Appendix II**), ε_{ctv} and ε_{ctd} can be calculated from x_v and x_m, where x_v and x_m are the medial-lateral lengths of the ventral and median fasciae, respectively. Therefore, for a given length of transverse aerobic muscle, one can, by varying the length of the median fascia through a reasonable range, find all arcs for that given length and, by determining which arc minimizes U, determine which arc will be observed.

Transverse muscle contraction proceeded by increments of 0·2% of original muscle length and ended when the arc of the fin subtended 90°. For each length of the contracting muscle, the length of the median fascia was allowed to range from 1·00001 times the length of the contracting muscle

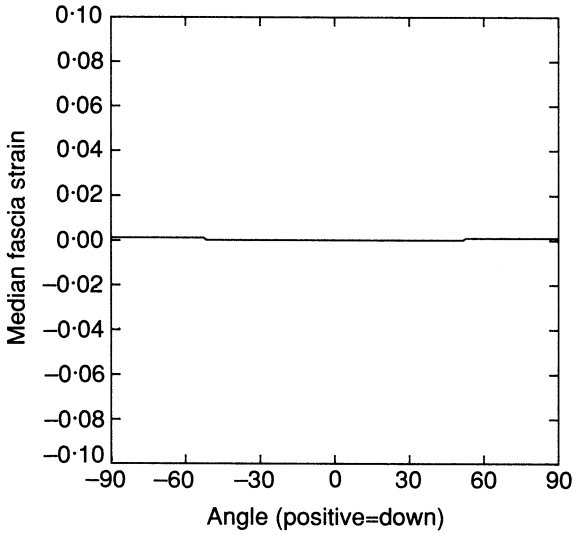

FIG. 9. Graph showing median fascia strain as a function of angle subtended by the arc of the fin during the simulation of bending.

to twice the original fascia length. The length of the median fascia could not exactly equal the length of the contracting muscle because of numerical overflow (see **Appendix II**).

The results can be seen in Figure 9. Note that the median fascia keeps an essentially constant length throughout a bend of 90°.

Appendix II

This appendix serves two purposes. First, it derives the map needed for the extension of the simulation of lateral compression to cases where the fin is bent. Secondly, it determines the relationships between the various dimensions of a bending beam as a function of the location of the neutral axis. This second part is used in the simulation of bending described in **Appendix I**.

Since the fin is a hydrostatic organ and since its transverse section is assumed to always be an arc (a straight line counting as an arc of infinite radius of curvature subtending 0°), it has only two degrees of freedom. Therefore, the value of two geometric parameters determine a unique configuration. In the extension of the simulation of lateral compression, R and x_m are the parameters given.

Let $c = x_o/y_o$, where x_o and y_o are the original medial-lateral and dorsoventral lengths of either prism. Figure 10 is the appropriate reference diagram.

$$(R-y_v)\phi = x_v, \tag{1}$$

$$R\phi = x_m, \tag{2}$$

$$(R+y_d)\phi = x_d. \tag{3}$$

From (1) and (2):

$$R = x_m y_v/(x_m - x_v) \quad \text{and} \quad \phi = (x_m - x_v)/y_v. \tag{4}$$

From (2) and (3):

$$R = x_m y_d/(x_m - x_v) \qquad \text{and} \qquad \phi = (x_d - x_m)/y_d. \tag{5}$$

Now, let A_v and A_d equal the areas of the large faces of the ventral and dorsal prisms, respectively. Basic trigonometry states:

$$A_v = \tfrac{1}{2}\phi(R^2 - (R - y_v)^2)$$

$$A_d = \tfrac{1}{2}\phi((R + y_d)^2 - R^2).$$

Using (4) and (5) gives:

$$A_v = \tfrac{1}{2} y_v (x_m + x_v), \tag{6}$$

$$A_d = \tfrac{1}{2} y_d (x_m + x_d). \tag{7}$$

Since A_v and A_d remain constant, $A_v = A_d = cy_o^2$.

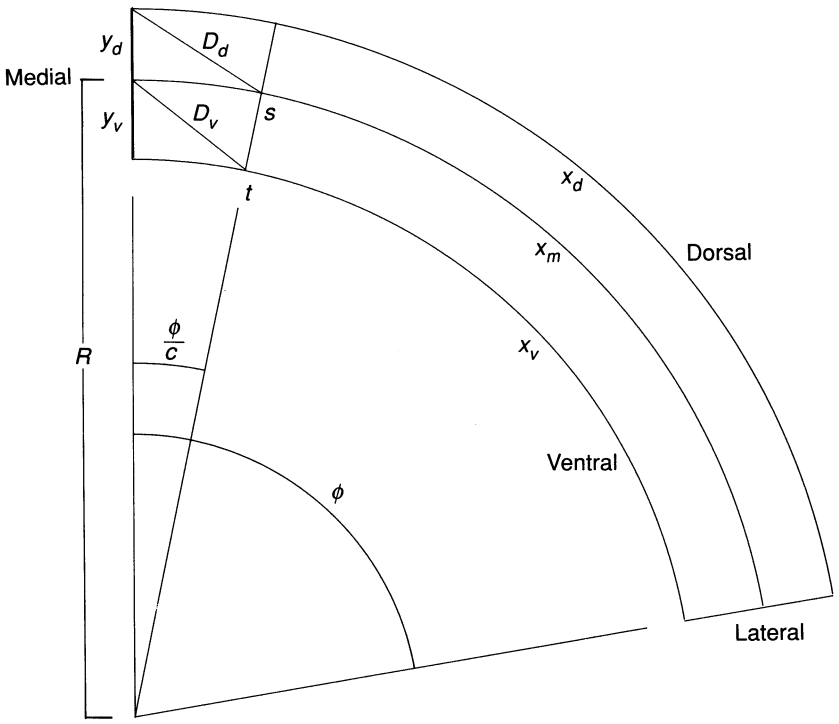

FIG. 10. Schematic diagram of the fin model bending ventrally. Only the diagonals nearest the fin base are shown. x_v, lateral length of the ventral surface of fin; x_d, lateral length of dorsal surface of fin; x_m, lateral length of median fascia; y_v, dorsoventral length of ventral half of the fin; y_d, dorsoventral length of dorsal half of the fin; D_v, length of a diagonal connective tissue fibre in the ventral half of the fin; D_d, length of a diagonal connective tissue fibre in the dorsal half of the fin; t, point where first ventral fibre meets ventral surface of fin; s, point where first dorsal fibre meets median fascia; R, radius of curvature of the fin's median fascia; ϕ, angle subtended by fin; c, twice the ratio of the medial-lateral to dorsoventral lengths of the fin.

Using this, one can solve (6) and (7) for y_v and y_d as:

$$y_v = 2cy_o^2/(x_v + x_m) \tag{8}$$

$$y_d = 2cy_o^2/(x_d + x_m). \tag{9}$$

(4) states:

$$\phi = (x_m - x_v)/y_v.$$

Using (8) to substitute for y_v gives:

$$x_v^2 = x_m^2 - 2\phi c y_o^2. \tag{10}$$

A similar use of (5) and (9) gives:

$$x_d^2 = x_m^2 + 2\phi c y_o^2. \tag{11}$$

Using (2), then (10) and (11), and then (8) and (9), one can calculate all the dimensions of the prism in terms of R and x_m.

From these dimensions, one can determine the lengths and therefore the strains of the connective tissue fibres in the dorsal and ventral prisms.

Using the coordinate system in Figure 10,

$$s_x = R\sin(\phi/c),$$

$$s_y = y_d + R(1 - \cos(\phi/c)),$$

$$t_x = (R - y_v)\sin(\phi/c), \qquad \text{and}$$

$$t_y = y_v + y_d + (R - y_v)(1 - \cos(\phi/c)).$$

The Pythagorean theorem gives:

$$D_v^2 = t_x^2 + (t_y - y_d)^2 \qquad \text{and} \qquad D_d^2 = s_x^2 + s_y^2.$$

The equations derived above can be used in the simulation of bending by using x_v and x_m, rather than x_m and ϕ, as the geometric parameters that determine the system.

Note that, though $R\phi = x_m$ at all times, when x_v is equal to x_m, R is infinite and ϕ is infinitesimal. Due to computational limitations in dealing with extremely large and small numbers, x_v is not allowed to equal x_m exactly in the simulations, though this is quite possible in actuality.

The calculations presented in this appendix are done only for the case in which the original fibre angle is 45°. The equations can be easily generalized to include other angles.

Appendix III

The kinetic energy of a bending fin section of constant lateral length

The total kinetic energy of the fin can be derived by calculating and then summing the kinetic energy of each point along the fin's lateral length. The most economical method is to calculate the kinetic energy of the point on the fin that is θ degrees from the fin base and then sum as θ ranges from 0 to ϕ.

$dK(\theta)$, the kinetic energy of the point at θ degrees from the fin base, equals $\frac{1}{2}\mathrm{dM}(u(\theta))^2$, where dM is the mass and $u(\theta)$ is velocity. $\mathrm{dM} = \mathrm{pdL}$, where p equals mass/length and L is the lateral length of the fin.

$dL = r d\theta$, where r is the radius of curvature of the fin. Therefore:

$$dK(\theta) = \tfrac{1}{2} p r d\theta (u(\theta))^2.$$

Before this can be integrated, we must derive the function that relates u and θ. If (x,y) is the point on the fin at angle θ, then

$$(u(\theta))^2 = (dx/dt)^2 + (dy/dt)^2.$$

Now,

$$x = r\sin\theta$$

$$y = r(1-\cos\theta).$$

By the chain rule of differentiation,

$$dx/dt = (dx/d\theta)(d\theta/dt)$$

$$dy/dt = (dy/d\theta)(d\theta/dt).$$

Differentiation gives:

$$dx/d\theta = (dr/d\theta)\sin\theta + r\cos\theta$$

$$dr/d\theta = (dr/d\theta)(1-\cos\theta) + r\sin\theta.$$

Therefore,

$$(dx/dt)^2 = ((dr/d\theta)^2\sin^2\theta + 2r(dr/d\theta)\sin\theta\cos\theta + r^2\cos^2\theta)(d\theta/dt)^2$$

$$(dy/dt)^2 = ((dr/d\theta)^2(1-2\cos\theta+\cos^2\theta) + r^2\sin^2\theta + 2(dr/d\theta)r\sin\theta(1-\cos\theta))(d\theta/dt)^2.$$

Adding and simplifying gives:

$$(u(\theta))^2 = (2((dr/d\theta)^2 + r(dr/d\theta)\sin\theta - (dr/d\theta)^2\cos\theta) + r^2)(d\theta/dt)^2.$$

Now the variables r, $dr/d\theta$, and $d\theta/dt$ must be given in terms of θ and constants. $r = b/\theta$, where b is the arc length from the fin base to angle θ.

Differentiating with respect to θ gives:

$$dr/d\theta = -b/\theta^2.$$

Note that r also equals L/θ, so $dr/d\theta = -L/(\theta\phi)$.

$$d\theta/dt = (b/L)(d\theta/dt).$$

Since $(L/\phi) = r = (b/\theta)$, $d\theta/dt = (\theta/\phi)(d\phi/dt)$

substitution gives:

$$(u(\theta))^2 = L^2(d\phi/dt)^2/\phi^4(\theta^2 + 2(1-\cos\theta-\theta\sin\theta)).$$

Now all that remains is to evaluate the integral.

$$\begin{aligned} K &= \tfrac{1}{2} p r \int_0^{\phi} (u(\theta))^2 d\theta \\ &= \tfrac{1}{2} p (d\phi/dt)^2 L^3/\phi^5 \int_0^{\phi} (\theta^2 + 2 - 2\cos\theta - 2\theta\sin\theta) d\theta \\ &= \tfrac{1}{2} p (d\phi/dt)^2 L^3/\phi^5 (\theta^3/3 + 2\theta + 2\theta\cos\theta - 4\sin\theta) \Big|_0^{\phi} \\ &= \tfrac{1}{2} p (d\phi/dt)^2 L^3/\phi^5 (\phi^3/3 + 2\phi + 2\phi\cos\phi - 4\sin\phi). \end{aligned}$$

This complicated expression can be accurately approximated and greatly simplified by the substitutions of the Taylor expansions of $\sin\phi$ and $\cos\phi$.

$$\sin\phi = \phi - \phi^3/3! + \phi^5/5! - \phi^7/7! \ldots$$

$$\cos\phi = 1 - \phi^2/2! + \phi^4/4! - \phi^6/6! \ldots$$

This gives:

$$K = \tfrac{1}{2}\mathrm{m}\mathrm{L}^2(\mathrm{d}\phi/\mathrm{d}t)^2/20.$$

Taylor series expansion of the trigonometric functions also greatly simplifies the expression for $u(\phi)$.

$$u(\phi) = \mathrm{L}^2(\mathrm{d}\phi/\mathrm{d}t)^2/\phi^4(\phi^2 + 2 - 2\cos\phi - 2\phi\sin\phi)$$

$$= \tfrac{1}{4}\mathrm{L}^2(\mathrm{d}\phi/\mathrm{d}t)^2.$$

Therefore K also equals $\mathrm{m}(u(\phi))^2/10$.